Experimental and Kinetic Modeling Study of the Pyrolysis and Oxidation of Decalin

ARTICLE *in* ENERGY & FUELS · MARCH 2009

Impact Factor: 2.79 · DOI: 10.1021/ef800892y

5 AUTHORS, INCLUDING:

Matthew A. Oehlschlaeger
Rensselaer Polytechnic Institute
77 PUBLICATIONS **1,610** CITATIONS
SEE PROFILE

Alessio Frassoldati
Politecnico di Milano
106 PUBLICATIONS **1,843** CITATIONS
SEE PROFILE

Sauro Pierucci
Politecnico di Milano
61 PUBLICATIONS **835** CITATIONS
SEE PROFILE

Eliseo Ranzi
Politecnico di Milano
225 PUBLICATIONS **4,772** CITATIONS
SEE PROFILE

Experimental and Kinetic Modeling Study of the Pyrolysis and Oxidation of Decalin

Matthew A. Oehlschlaeger,[†] Hsi-Ping S. Shen,[†] Alessio Frassoldati,[‡] Sauro Pierucci,[‡] and Eliseo Ranzi*,[‡]

Mechanical, Aerospace, and Nuclear Engineering, Rensselaer Polytechnic Institute, Troy, New York 12180, and CMIC Department, Politecnico di Milano, Piazza Lenoardo da Vinci 32, Milano 20133, Italy

Received October 15, 2008. Revised Manuscript Received December 16, 2008

Decalin is a model compound for bicyclic naphthenes found in jet fuels and coal-, oil-shale-, tar-sand-derived fuels, and it is also a potential endothermic fuel for hypersonic flight. Additionally, decalin is a reference component in surrogate mixtures of jet fuels. New shock tube ignition delay time measurements have been performed for decalin/air mixtures at elevated-pressure conditions relevant to practical combustion engines for varying pressure (9−15 and 35−48 atm), equivalence ratio ($\Phi = 0.5$ and 1.0), and temperature (990−1300 K). An automatic kinetic generator, the MAMA code, has been applied to develop a semi-detailed submechanism for decalin decomposition at high-temperature conditions. Kinetic simulations are compared to the measured ignition times with adequate agreement. Sensitivity analysis indicates limited importance of decalin unimolecular decomposition and hydrogen abstraction from decalin and moderate importance of the decomposition of $C_{10}H_{17}$ radicals in predicting ignition times. The new decalin submechanism further advances the kinetic understanding of pyrolysis and oxidation of heavy hydrocarbons found in practical fuels.

Introduction

Because of the chemical complexity of commercial distillate jet fuels (e.g., Jet A and JP-8), surrogate jet fuel mixtures made up of a limited number of hydrocarbon compounds are desired.[1] Surrogate mixtures are typically designed to mimic the physical and/or chemical properties of commercial fuels. Chemical surrogates may be designed to capture the laminar burning velocity, high-temperature autoignition, low-temperature oxidation, and pollutant and soot formation tendencies of the complex distillate fuel at a range of conditions. The development of surrogate mixtures enables the simulation of combustion processes using chemistry describing only the oxidation of the surrogate mixture and not the thousands of compounds contained in the complex distillate fuel. Additionally, surrogate mixtures allow for a direct comparison of simulations to experiments carried out using the surrogate. The development of surrogate representations is also useful for the investigation of the influence that fuel composition and properties have on combustion processes.

The chemical composition of jet fuels varies depending upon the crude source, refinery, time of year, and age of the fuel. However, on average, jet fuels are made up of ∼30% iso-paraffins, ∼30% *n*-paraffins, ∼20% naphthenes, and ∼20% aromatics, with minor amounts of olefins, naphthalenes, and other hydrocarbons.[1−3] Surrogate mixtures for jet fuels are usually made up of representative compounds from these hydrocarbon classes. The oxidation kinetics of these hydrocarbon classes have been investigated to varying degrees, with the paraffins having been studied the most extensively, particularly the C_8 and smaller compounds, and the aromatics and naphthenes having been studied to a lesser degree. In particular, there have been few kinetic studies of bicyclic naphthenes, including decalin ($C_{10}H_{18}$, decahydronaphthalene).

Decalin occurs in both *cis* and *trans* isomers, of which the *trans* is energetically more stable and has a lower boiling point. Decalin has received interest as a multi-ring naphthene class surrogate mixture component for jet fuels.[2,4−13] For example, Eddings et al.[12] used decalin at up to 35% in surrogate mixtures

* To whom correspondence should be addressed: CMIC Department, Politecnico di Milano, Piazza Lenoardo da Vinci 32, Milano 20133, Italy. Telephone: +39-02-23993250. Fax: +39-02-70638173. E-mail: eliseo.ranzi@polimi.it.

[†] Rensselaer Polytechnic Institute.

[‡] Politecnico di Milano.

(1) Colket, M.; Edwards, J. T.; Williams, S.; Cernansky, N. P.; Miller, D. L.; Egolfopoulos, F. N.; Lindstedt, P.; Seshadri, K.; Dryer, F. L.; Law, C. K.; Friend, D. G.; Lenhert, D. B.; Pitsch, H.; Sarofim, A.; Smooke, M.; Tsang, W. American Institute of Aeronautics and Astronautics (AIAA) Paper AIAA-2007-0770, 2007.

(2) Edwards, T.; Maurice, L. Q. *J. Prop. Power* **2001**, *17*, 461–466.

(3) Shafer, L.; Striebich, R.; Gomach, J.; Edwards, T. American Institute of Aeronautics and Astronautics (AIAA) Paper AIAA-2006-7972, 2006.

(4) Wood, C. P. The development and application of surrogate blends in simulating the combustion performance of distillate aviation fuels. M.S. Thesis, University of California, Irvine, CA, 1989.

(5) Wood, C. P.; McDonell, V. G.; Smith, R. A.; Samuelsen, G. S. *J. Prop. Power* **1989**, *5*, 399–405.

(6) Schulz, W. D. *Prepr. Pap.−Am. Chem. Soc., Div. Pet. Chem.* **1991**, *37*, 383–392.

(7) Edwards, T. American Institute of Aeronautics and Astronautics (AIAA) Paper AIAA-93-0807, 1993.

(8) Violi, A.; Yan, S.; Eddings, E. G.; Sarofim, A. F.; Granata, S.; Faravelli, T.; Ranzi, E. *Combust. Sci. Technol.* **2002**, *174*, 399–417.

(9) Agosta, A. Development of a chemical surrogate for JP-8 aviation fuel using a pressurized flow reactor. M.S. Thesis, Drexel University, Philadelphia, PA, 2002.

(10) Agosta, A.; Lenhert, D. B.; Miller, D. L.; Cernansky, N. P. Development and evaluation of a JP-8 surrogate that models preignition behavior in a pressurized flow reactor. Presented at the 3rd Joint Meeting of the U.S. Sections of the Combustion Institute, 2003.

(11) Agosta, A.; Cernansky, N. P.; Miller, D. L.; Faravelli, T.; Ranzi, E. *Exp. Therm. Fluid Sci.* **2004**, *28*, 701–708.

(12) Eddings, E. G.; Yan, S.; Ciro, W.; Sarofim, A. F. *Combust. Sci. Technol.* **2005**, *177*, 715–739.

(13) Ranzi, E. *Energy Fuels* **2006**, *20*, 1024–1032.

10.1021/ef800892y CCC: $40.75
Published on Web 01/29/2009

to predict the sooting tendencies of JP-8 pool fires, and Agosta[9] included decalin in a JP-8 surrogate at 6% by volume to match the low-temperature reactivity. Additionally, decalin is attractive as an endothermic propulsion fuel or fuel additive, potentially enabling cooling systems for hypersonic flight that use both chemical and sensible energy absorption.[14,15] Decalin is attractive as an endothermic propulsion fuel because of its high thermal stability[16] and because, as a hydrogen donor, it suppresses carbon deposits when pyrolyzed, preventing fouling of fuel delivery systems.[14,17] Decalin is also a model compound for coal-, oil-shale-, and tar-sand-derived jet fuels, which contain large fractions of bicyclic naphthenes.[3]

Previous kinetic studies related to decalin have primarily focused on its pyrolysis.[18−27] Decalin pyrolysis studies have been carried out at a range of pressures from below atmospheric to supercritical in flow reactors,[14,19,20,22,23,25] very low-pressure pyrolysis reactors,[24] static reactors,[18,25] and steam cracking flow reactors[21] and using laser-induced decomposition.[23] These studies have identified the major products of decalin pyrolysis for different conditions. The lower pressure pyrolysis studies of Ondruschka et al.[23] (770−1020 K), Hillebrand et al.[20] (973−1123 K), and Billaud et al.[21] (1083 K) found the products of decalin pyrolysis to include methane, C_2-C_4 alkenes (ethylene, propene, and butadiene), benzene, toluene, xylenes, styrene, 3-methylenecyclohexene, and other aromatics. Stewart et al.[14] at supercritical pressures (40.9 atm) indentified C_2-C_4 alkenes, benzene, and toluene as products at higher temperatures (∼810 K), similar to the findings of the lower pressure studies, but observed different products at lower temperatures (∼730 K), including light alkanes, methylhexahydroindane, indene, indane, and methylenecyclohexane. Stewart et al. explained the formation of the more compact products at the lower temperatures of their supercritical pressure study through C_6-C_5 ring contractions because of caging effects similar to those that occur in liquids. Zhu et al.[26] in oxidative decalin cracking experiments identified C_2-C_4 alkenes, alkylbenzenes, alkylcyclohexanes, and iso-paraffins as primary products at temperatures around 873 K and C_2-C_4 alkenes, benzene, toluene, and xylenes as primary products at temperatures around 1073 K. Chae and Violi[27] have recently investigated the thermal decomposition of decalin using *ab initio* techniques at temperatures ranging from 700 to 1500 K. Their calculations predict the primary products of decalin decomposition in the high-pressure limit to be monoaromatic species and C_2-C_4 radicals, which under high-temperature conditions will thermally decompose rapidly to C_2-C_4 alkenes. Benzene and toluene are produced through multiple pathways, and their concentrations in the products are significant (64−94% benzene and 6−31% toluene depending upon the temperature). Xylene as well as styrene and ethylbenzene are only produced in small quantities (<0.5%). According to Chae and Violi,[27] decomposition products from decalin are obtained through carbon−carbon bond cleavage, dissociation, and hydrogen abstraction.

There are fewer previous studies found in the literature focused on the oxidation of decalin rather than its pyrolysis. Nixon et al.[28] studied the high-temperature ignition of decalin in a shock tube at low pressures (0.6−1.5 atm), for fuel dilute decalin/O_2/Ar mixtures containing 80 or 90% Ar on a molar basis at equivalence ratios of $\Phi = 0.1$ and 0.2 and for temperatures ranging from 1060 to 1290 K. More recently, Agosta[9] studied the reactivity of decalin in the negative temperature coefficient (NTC) regime.

To our knowledge, the kinetic modeling study of Ranzi[13] is the only previously published kinetic mechanism describing the oxidation of decalin. The mechanism uses a lumped reaction scheme to describe the decomposition of decalin. One lumped intermediate radical, formed via a hydrogen atom abstraction reaction from decalin, simply decomposes at high temperature by β-scission reactions. These lumped decalin reactions are tied to a semi-detailed oxidation reaction mechanism for alkanes, alkenes, and aromatics up to C_{16}, which describes the oxidation and decomposition of the decalin decomposition products.

In response to the absence of previous kinetic studies related to the oxidation and ignition of decalin, particularly at conditions of elevated pressure of relevance to aero-propulsion applications, here, we present new shock-tube measurements of decalin ignition in air mixtures at elevated pressures and a further refinement of the kinetic mechanism for the description of the high-temperature pyrolysis and oxidation of decalin that includes extensions and modifications to the previous mechanism.[13] Kinetic simulations are compared to the measured ignition times with adequate agreement. Sensitivity analysis indicates the importance of hydrogen atom abstraction from decalin to form $C_{10}H_{17}$ radicals and the decomposition of the $C_{10}H_{17}$ radicals in predicting ignition times. Sensitivity is also shown for reactions from the C_0-C_2 database, with ignition times showing strong sensitivity to hydrogen peroxide decomposition ($OH + OH + M \leftrightarrow H_2O_2 + M$) and the reaction of hydroperoxyl radicals ($HO_2 + HO_2 \leftrightarrow H_2O_2 + O_2$).

Kinetic Modeling

A semi-detailed kinetic mechanism for the description of the high-temperature oxidation and pyrolysis of decalin is discussed and presented here. This mechanism is based on lumped reactions and species for simplified description of the formation of decalin decomposition products. The further decomposition and/or oxidation of these smaller radicals and molecules is described in a semi-detailed oxidation mechanism for hydrocarbon fuels up to C_{16} developed in previous works.[13,29] The overall kinetic scheme is based on hierarchical modularity and is constituted by more than 300 species involved in more than 7000 reactions. Thermochemical data for most species were obtained from the CHEMKIN thermodynamic database;[30,31] unavailable thermodynamic data were estimated

(14) Stewart, J.; Brezinsky, K.; Glassman, I. *Combust. Sci. Technol.* **1998**, *136*, 373–390.
(15) Lander, H.; Nixon, A. C. *J. Aircraft* **1971**, *8*, 200–207.
(16) Gollis, M. H.; Belenyessy, L. I.; Gudzinowicz, B. J.; Koch, S. D.; Smith, J. O.; Wineman, R. J. *J. Chem. Eng. Data* **1962**, *7*, 311–316.
(17) Corporan, E.; Minus, D. K.; Williams, T. F. Studies of decalin as a suppressor of pyrolytic deposits in JP-8 + 100. Presented at the 35th AIAA Joint Prolusion Conference, 1999.
(18) Fabuss, B. M.; Kafesjian, R.; Smith, J. O.; Satterfield, C. N. *Ind. Eng. Chem. Process Des. Dev.* **1964**, *3*, 248–254.
(19) Bredael, P.; Rietvelde, D. *Fuel* **1979**, *58*, 215–218.
(20) Hillebrand, W.; Hodek, W.; Kolling, G. *Fuel* **1984**, *63*, 756–761.
(21) Billaud, F.; Chaverot, P.; Freund, E. *J. Anal. Appl. Pyrolysis* **1987**, *11*, 39–53.
(22) Taylor, P. H.; Rubey, W. A. *Energy Fuels* **1988**, *2*, 723–728.
(23) Ondruschka, B.; Zimmermann, G.; Remmler, M. *J. Anal. Appl. Pyrolysis* **1990**, *18*, 19–32.
(24) Ondruschka, B.; Zimmermann, G.; Remmler, M. *J. Anal. Appl. Pyrolysis* **1990**, *18*, 33–39.
(25) Yu, J.; Eser, S. *Ind. Eng. Chem. Res.* **1998**, *37*, 4601–4608.
(26) Zhu, H.; Liu, X.; Ge, Q.; Li, W.; Xu, H. *Fuel Process. Technol.* **2006**, *87*, 649–657.
(27) Chae, K.; Violi, A. *J. Org. Chem.* **2007**, *72*, 3179–3185.
(28) Nixon, A. C.; Ackerman, G. H.; Faith, L. E.; Hawthorn, R. D.; Henderson, H. T.; Ritchie, A. W.; Ryland, L. B. Vaporizing and endothermic fuels for advanced engine applications. U.S. Air Force Technical Report AFAPL-RF-67-114, 1967.
(29) Ranzi, E.; Dente, M.; Bozzano, G.; Goldaniga, A.; Faravelli, T. *Prog. Energy Combust. Sci.* **2001**, *27*, 99–139.
(30) Kee, R. J.; Rupley, F.; Miller, J. A. The Chemkin Thermodynamic Data Base. Report SAND86-8215B, Sandia National Laboratories, Albuquerque, NM, 1987.

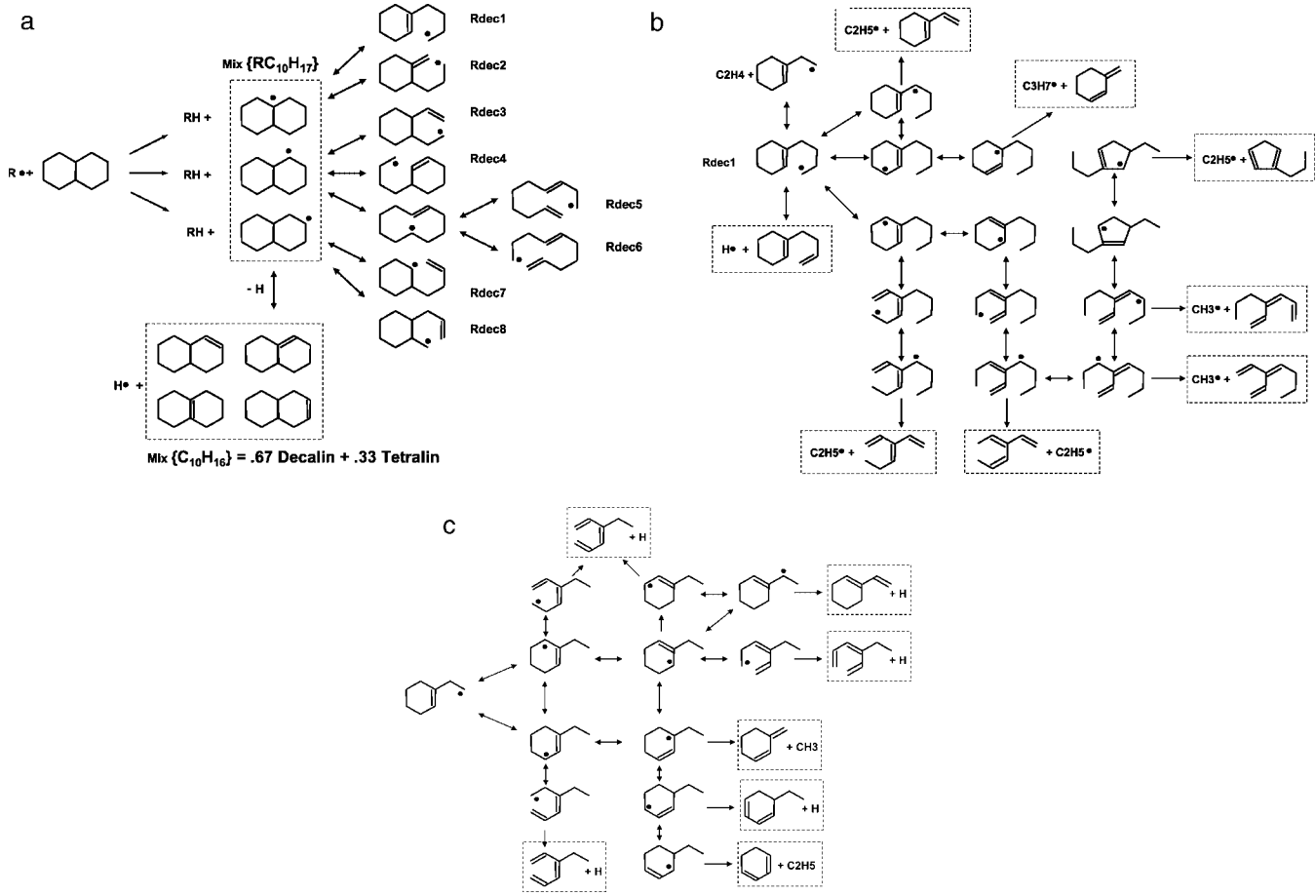

Figure 1. (a) Hydrogen abstraction reactions on decalin and primary decomposition and dehydrogenation reactions. (b) Isomerization and decomposition reactions of the radical Rdec1. (c) Successive isomerization and decomposition reactions of the radical C_8H_{13}.

using the group additivity method.[32] The complete mechanism is available online at (www.chem.polimi.it/CRECKModeling/).

The automatic generation of a semi-detailed kinetic model for the high-temperature decomposition of decalin has been performed using the MAMA program previously described by Dente et al.[33] and Pierucci and Ranzi.[34] The main functions of the MAMA program are shortly summarized in the Appendix, together with further details on the products of decalin decomposition.

Because of the symmetry of the structure of decalin, hydrogen abstraction from decalin can result in the formation of three $C_{10}H_{17}$ radicals (Figure 1a). At high temperature ($T > 1000$ K), these three primary $C_{10}H_{17}$ radicals can isomerize and decompose to form eight different $C_{10}H_{17}$ radicals. The successive isomerization and decomposition of these radicals is very complex and requires the use of automated techniques for the determination of reaction paths and product fractions. The lifetime of the $C_{10}H_{17}$ radicals is less than 10^{-6} s at high temperatures ($T > 1000$ K), and it is convenient to lump their multistep decomposition and directly analyze their primary decomposition products. Figure 1b shows only a sample of the possible isomerization and decomposition paths for the Rdec1 radical. To clarify the complexity of the overall decomposition mechanism, Figure 1c shows a limited portion of the possible isomerization and decomposition paths of the C_8H_{13} radical, formed at significant concentrations from β-scission of the Rdec1 radical, which results in ethylene and the C_8H_{13} radical. A very recent kinetic study of Tsang on cyclo-hexyl radical reactions gives and confirms several reference kinetic parameters of elementary isomerization, ring-opening, and cyclization reactions.[35]

To illustrate the need for lumped species and reactions, a complete description of the primary decomposition of the C_8H_{13} radical, as formulated by the MAMA program, involves approximately 3000 isomerization and decomposition reactions and more than 800 radicals and molecular species. A complete description of the decomposition of the decalin would require more than 75 000 reactions and 5500 species. It is evident, from the extremely large number of species and reactions that are required for a detailed description of the decomposition of decalin, that the results of a kinetic generator are of no practical use in the detailed form that they are obtained. However, tractable kinetic mechanisms can be formulated by "lumping" the components using certain preassigned rules, which satisfy the requirements of the reactor model for which kinetic simulations will be performed. Additional details regarding kinetic lumping can be found in the Appendix.

On the basis of a limited set of independent kinetic parameters and after the necessary lumping phase, the MAMA program evaluates the product distribution of thermal decomposition at a fixed temperature. For example, at 1000 K, the predicted distribution of the decomposition products of C_8H_{13} is

$$C_8H_{13} \rightarrow 0.22(H + C_8H_{12}) + 0.678(CH_3 + C_7H_{10}) + 0.11(RcyC_6H_9 + C_2H_4) + 0.04(aC_3H_5 + C_5H_8) + 0.011(C_2H_5 + cyC_6H_8)$$

It is relevant to observe that the MAMA code reports the detail of the different C_7H_{10} and C_8H_{12} isomers. As shown in parts b and

(31) Kee, R. J.; Rupley, F.; Miller, J. A. The Chemkin Thermodynamic Data Base. Sandia National Laboratories, Albuquerque, NM, 1989.
(32) Benson, S. W. *Thermochemical Kinetics*, 2nd ed.; Wiley: New York, 1976.
(33) Dente, M.; Bozzano, G.; Faravelli, T.; Marongiu, A.; Pierucci, S.; Ranzi, E. *Adv. Chem. Eng.* **2007**, *32*, 52–168.
(34) Pierucci, S.; Ranzi, E. *Comput. Chem. Eng.* **2008**, *32*, 805–826.
(35) Tsang, W. Prime: A database for the pyrolysis of heptane and samller hydrocarbons fuels; implications for realistic fuels. Work-in-progress poster at the 32nd International Symposium on Combustion, Montreal, Canada, Aug 3−8, 2008.

c of Figure 1, C_8H_{12} is a lumped mixture of different isomers, including ethyl-hexatriene, vinyl-hexadiene, and vinyl-cyclohexene, while C_7H_{10} is a significant precursor of benzene and toluene. Additionally, the β-scission of C_8H_{13} radicals forms ethylene and cyclohexenyl radicals at significant fractions. The MAMA program also predicts allyl radical and isoprene production, as a result of successive isomerization reactions. Minor product fractions (less than 1% molar) of iso- and n-C_4H_7 and cyclopentenyl (C_5H_7) radicals as well as butadiene and cyclopendadiene are not accounted in the reported simplified lumped C_8H_{13} radical decomposition. The influence of the temperature on the distribution of intermediate products is limited and does not affect, in a significant way, the relative importance of the different reaction paths and the characteristics of the reacting system, as discussed by Dente et al.[33] For instance, the decomposition of the C_8H_{13} radical at 1100 K yields product fractions similar to those given above for 1000 K. Details on these product distributions are given in the Appendix.

Similarly, at 1000 K, the overall decomposition products from the Rdec1 radical predicted using the MAMA program and truncated to neglect several very minor products are

$$\begin{aligned}\text{Rdec1} \rightarrow 0.088(\text{H} + \text{C}_2\text{H}_4 + \text{C}_8\text{H}_{12}) + 0.014(\text{H} + \text{C}_3\text{H}_6 + \text{C}_7\text{H}_{10}) + 0.073(\text{H} + \text{C}_4\text{H}_8 + \text{C}_6\text{H}_8) + 0.41(\text{CH}_3 + \text{C}_2\text{H}_4 + \text{C}_7\text{H}_{10}) + 0.03(\text{CH}_3 + \text{C}_3\text{H}_6 + \text{C}_6\text{H}_8) + 0.184(\text{C}_2\text{H}_5 + \text{C}_8\text{H}_{12}) + 0.066(\text{C}_3\text{H}_7 + \text{C}_7\text{H}_{10}) + 0.005(\text{C}_3\text{H}_5 + \text{C}_7\text{H}_{12}) + 0.03(\text{C}_3\text{H}_5 + \text{C}_2\text{H}_4 + \text{C}_5\text{H}_8) + 0.001(\text{C}_5\text{H}_7 + \text{C}_2\text{H}_4 + \text{C}_3\text{H}_6) + 0.074(2\text{C}_2\text{H}_4 + \text{RcyC}_6\text{H}_9)\end{aligned}$$

Kinetic analysis of the product distributions for the decomposition of the eight different radicals reported in Figure 1a has been performed using the MAMA program. The final product distribution for the decomposition of the lumped combination of the $C_{10}H_{17}$ radicals becomes

$$\begin{aligned}\text{mix}\{\text{RC}_{10}\text{H}_{17}\} \rightarrow 0.025(\text{H} + \text{C}_{10}\text{H}_{16}) + 0.033(\text{H} + \text{C}_2\text{H}_4 + \text{C}_8\text{H}_{12}) + 0.011(\text{H} + \text{C}_3\text{H}_6 + \text{C}_7\text{H}_{10}) + 0.037(\text{H} + \text{C}_4\text{H}_8 + \text{C}_6\text{H}_8) + 0.01219(\text{H} + \text{C}_4\text{H}_6 + \text{C}_6\text{H}_{10}) + 0.117(\text{CH}_3 + \text{C}_4\text{H}_6 + \text{C}_5\text{H}_8) + 0.109(\text{CH}_3 + \text{C}_2\text{H}_4 + \text{C}_7\text{H}_{10}) + 0.023(\text{CH}_3 + \text{C}_3\text{H}_6 + \text{C}_6\text{H}_8) + 0.032(\text{CH}_3 + 2\text{C}_2\text{H}_4 + \text{C}_5\text{H}_8) + 0.040(\text{CH}_3 + \text{C}_4\text{H}_8 + \text{C}_5\text{H}_6) + 0.122(\text{C}_2\text{H}_5 + \text{C}_8\text{H}_{12}) + 0.018(\text{C}_2\text{H}_5 + 2\text{C}_4\text{H}_6) + 0.064(\text{C}_3\text{H}_7 + \text{C}_7\text{H}_{10}) + 0.075(\text{C}_3\text{H}_5 + \text{C}_7\text{H}_{12}) + 0.059(\text{C}_3\text{H}_5 + \text{C}_2\text{H}_4 + \text{C}_5\text{H}_8) + 0.011(\text{C}_3\text{H}_5 + \text{C}_3\text{Hy} + \text{C}_4\text{H}_6) + 0.069(\text{C}_4\text{H}_7 + \text{C}_6\text{H}_{10}) + 0.016(\text{C}_4\text{H}_7 + \text{C}_2\text{H}_4 + \text{C}_4\text{H}_6) + 0.072(2\text{C}_2\text{H}_4 + \text{RcyC}_6\text{H}_9)\end{aligned}$$

Once again, several product fractions less than 1% are not reported. The above product distribution is predicted by the MAMA code using the hypothesis that large radicals decompose to form more stable radicals and smaller molecules. This distribution requires further simplification to be implemented in the overall kinetic scheme. A total of 13 decomposition reactions are used to describe the overall decomposition of the lumped mix{$RC_{10}H_{17}$} radical, maintaining the relative importance of the different reaction paths as predicted by the MAMA code. We assume an overall decomposition rate constant of 3.5×10^{13} exp(−30 000 (kcal/kmol)/RT) (s^{-1}); these are typical reference kinetic parameters of β-decomposition reactions of alkyl radicals. Kinetic parameters for the different decomposition reactions are simply scaled on the basis of the relative reaction flux for the different reaction paths. Table A3 in the Appendix reports the small subset of lumped reactions used to describe decalin decomposition. These lumped decalin reactions are tied to the overall semi-detailed oxidation mechanism, which describes the fate of the decalin decomposition products.

To verify the predicted decalin decomposition product distribution, the pyrolysis experiments of Ondruschka et al.[23] have been simulated. At 1020 K, parts a and b of Figure 2 show the predicted selectivities of H_2 and C_1−C_4 gases and heavier components as a function of the contact time. Selectivities are defined as the formed moles of decomposition products per mole of decalin consumed. The kinetic predictions for the decomposition product distribution are in close and satisfactory agreement with the experimental measurements of Ondruschka et al.[23] It is also important to observe that benzene is not a primary product. Rather, its relevant formation is the result of successive reactions. According to our scheme, reaction path analysis shows that benzene formation is due to dehydrogenation of cyclohexadiene, successive reactions of cyclopentadiene, as well as dealkylation of toluene and heavy aromatics. This successive formation of benzene fully agrees with the experimental data of Ondruschka et al.[23] They measure benzene selectivity lower than 0.05 at decalin conversion up to 20%, and only then, they observe a rising selectivity when decalin conversion increases. Ondruschka et al.[23] observed selectivity of 3-methylencyclohexene greater than 35%. Parts b and c of Figure 1 show the corresponding reaction paths for methyl and 1-propyl radical formation, respectively. The initial selectivity of toluene and C_8 aromatics is only due to the lack of heavy intermediate components (C_nH_{2n-2} and C_nH_{2n-4}) and to the assumption of direct dehydrogenation with aromatic formation. Further details regarding this simplification are given in the Appendix.

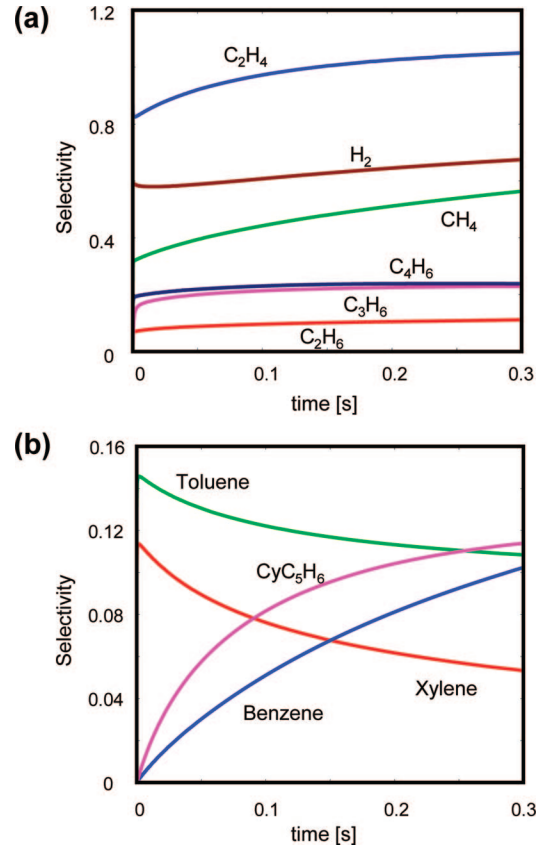

Figure 2. (a) Predicted selectivities of gases versus the contact time for decalin pyrolysis at 1 bar and 1020 K. (b) Predicted selectivities of cyclo-pentadiene and aromatics versus the contact time for decalin pyrolysis at 1 bar and 1020 K.

Experimental Method and Results

Decalin ignition times were measured in the externally heated high-pressure shock tube at Rensselaer Polytechnic Institute, previously described in ignition studies of cyclopentane and cyclohexane[36] and methyl-cyclohexane and ethyl-cyclohexane.[37] For the current experiments, the shock tube and mixing manifold and vessel were heated to a temperature of 80 °C to provide sufficient decalin vapor pressure for high-pressure experiments. The shock-tube temperature uniformity was routinely monitored, with non-uniformity within ±2 °C. Decalin/air mixtures at

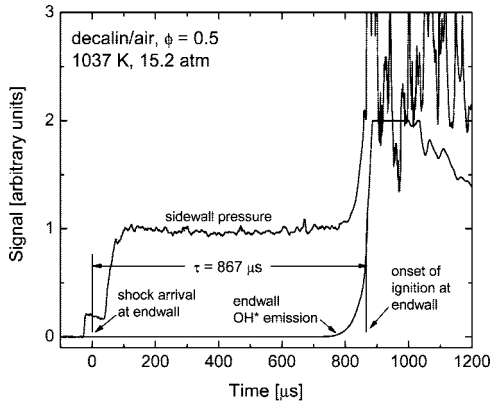

Figure 3. Example decalin/air ignition time measurement.

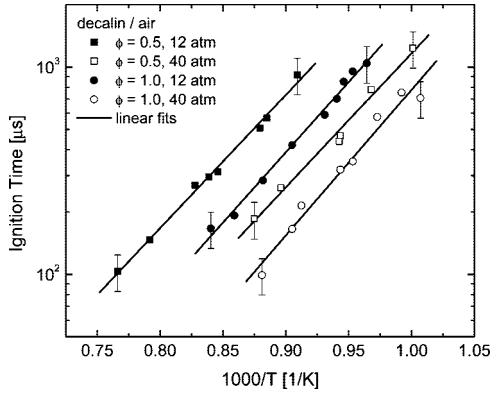

Figure 4. Ignition time results for decalin/air mixtures at $\Phi = 0.5$ and 1.0. Results scaled to 12 and 40 atm to account for deviations in reflected shock pressures using $\tau \propto P^{-0.78}$.

equivalence ratios of 0.5 and 1.0 were prepared using a 99+% pure mixture of *trans* and *cis* decalin from Sigma Aldrich and O_2 at 99.995% purity and N_2 at 99.995% purity. The decalin was degassed prior to mixture preparation and introduced to the mixing vessel via vaporization.

Ignition times were determined in the reflected shock region using electronically excited OH emission viewed through the shock-tube endwall and pressure measurements made using a piezoelectric transducer located in the sidewall at a location 2 cm from the endwall. Reflected shock conditions were determined using the standard normal shock relations, with thermodynamic data for decalin taken from that used in the kinetic mechanism described above. The uncertainty in the reflected shock temperatures and pressure are estimated at 1.5 and 2.0%, respectively. Ignition times were measured for $\Phi = 0.5$ and 1.0 decalin/air mixtures for temperatures ranging from 993 to 1305 K and pressures falling into two ranges from 9.3 to 15.2 atm and from 34.6 to 48.0 atm. These conditions were chosen for their relevance to elevated-pressure combustion in practical devices (turbines, IC engines, etc.) and because of their accessibility in the shock tube. Rich conditions were not considered to avoid experimental complications inherent with soot formation and contamination of the shock tube. An example ignition time measurement is shown in Figure 3.

The ignition time data are displayed on Arrhenius axes in Figure 4 and are given in Table 1. In the temperature range investigated, the ignition time measurements show exponential dependence upon the inverse temperature, with no indication of NTC behavior. Additionally, the ignition times decrease with an increasing pressure and equivalence ratio, typical of hydrocarbon fuels at elevated pressure for equivalence ratios from lean to stoichiometric.[36,37] The ignition time results are characterized by little scatter about the linear least-squares fits shown in Figure 4 (±10%). The uncertainty is estimated at ±20% in ignition time based on combined uncertainties in reflected shock temperature and pressure and their temporal variation because of non-ideal gas dynamics, reactant mixture composition, and the uncertainty in determining the ignition time from the measured pressure and emission signals.

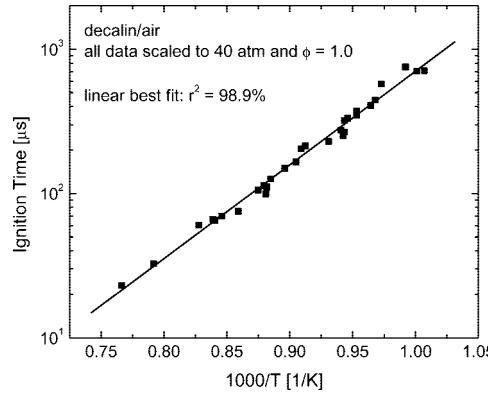

Figure 5. Ignition times scaled to a common condition of 40 atm and $\Phi = 1.0$ using the correlation given in the text.

Table 1. Measured Ignition Times for Decalin/Air Mixtures

decalin/air ($\Phi = 0.5$)			decalin/air ($\Phi = 1.0$)		
P (atm)	T (K)	τ (μs)	P (atm)	T (K)	τ (μs)
13.5	1100	837	15.2	1037	867
12.0	1130	567	13.5	1049	871
12.1	1137	505	12.5	1057	825
11.6	1182	321	13.9	1063	627
12.1	1192	294	12.2	1074	580
11.1	1208	287	14.1	1105	371
10.6	1263	161	10.5	1134	315
10.7	1305	113	11.4	1164	200
42.1	999	1186	9.3	1190	203
44.5	1033	717	34.6	993	793
41.4	1060	455	48.0	1008	654
37.2	1061	464	46.7	1028	509
37.0	1116	279	41.6	1049	340
35.8	1143	202	42.6	1060	305
			44.6	1096	197
			41.8	1105	160
			38.1	1135	103

The measured ignition times can be correlated using Arrhenius temperature dependence and power-law dependence on the pressure and equivalence ratio resulting in

$$\tau = 4.05 \times 10^{-9} P^{-0.78} \Phi^{-0.81} \exp(14930/T\,(\mathrm{K}))\ (\mathrm{s})$$

where τ is the ignition time in seconds, T the temperature in Kelvin, and P the pressure in atm. The ignition times are shown scaled to a common condition (40 atm and $\Phi = 1.0$) in Figure 5, illustrating the adequacy of the correlation for representing the data over the range of experimental conditions ($r^2 = 98.9\%$ for the best fit in Figure 5). Additionally, the data presented in Figure 5 have been scaled to 12 and 40 atm to account for deviations in reflected shock pressure using the power-law pressure scaling given above.

To our knowledge, there have been no previous decalin ignition delay time measurements at conditions similar to those investigated here for comparison to the current study.

Comparison, Sensitivity Analysis, and Discussion

Figure 6 shows the comparisons of measured ignition times with predictions from the new decalin mechanism. Kinetic

(36) Daley, S. M.; Berkowitz, A. M.; Oehlschlaeger, M. A. *Int. J. Chem. Kinet.* **2008**, *40*, 624–634.

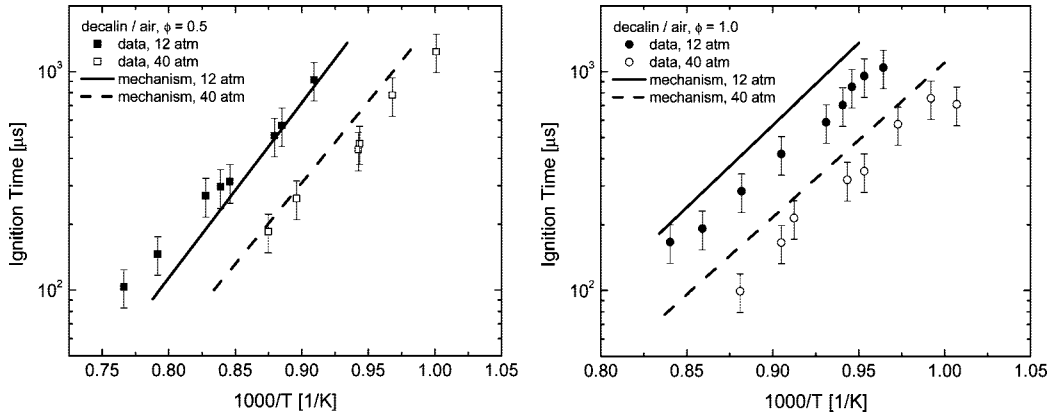

Figure 6. Comparison of measured ignition times with mechanism predictions.

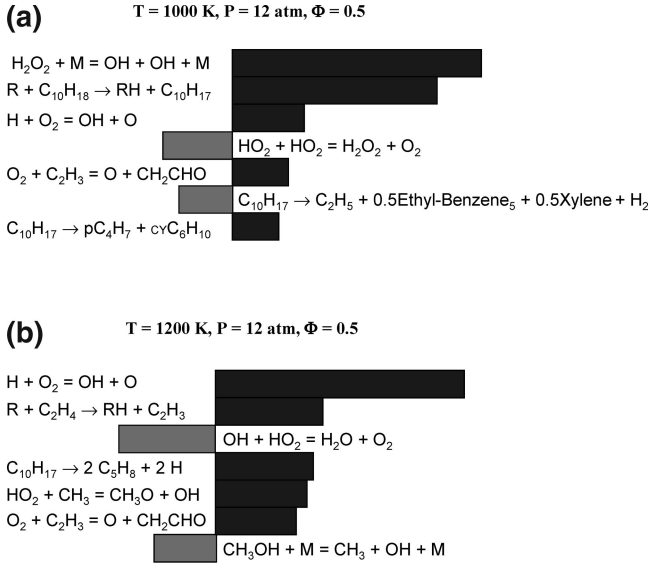

Figure 7. (a) Sensitivity analysis for OH radical formation at $T = 1000$ K. Dark bars indicate positive sensitivity coefficients. (b) Sensitivity analysis for OH radical formation at $T = 1200$ K. Dark bars indicate positive sensitivity coefficients.

simulations were carried out using the closed homogeneous constant-volume reactor model commonly used to model the reflected shock region. The kinetic predictions are in good agreement at $\Phi = 0.5$, while ignition times are overpredicted by 20−40% at $\Phi = 1.0$. We consider this to be good agreement in light of the kinetic complexity of decalin oxidation and because the mechanism was developed *a priori* with no adjustments to rate parameters to fit data.

Sensitivity analysis has been performed at a variety of stoichiometries, temperatures, and pressures. The results are briefly summarized in parts a and b of Figure 7. At 1000 K, the analysis shows that, together with the H_2O_2 decomposition, the hydrogen abstraction reactions for decalin show the greatest sensitivity and increasing the rate coefficients for these reactions has a promoting influence on the overall reactivity (decreases ignition time). The sensitivity analysis also shows that the decomposition of $C_{10}H_{17}$ to form ethyl radicals and C_8 aromatics (ethylbenzene and xylenes) has an inhibiting effect on reactivity, while the decomposition path to form cyclohexane and C_4H_7 radicals has a promoting influence. This effect, more pronounced at high pressure, seems mainly because of the adopted simplifications of the lumped kinetic scheme. The assumed direct and instantaneous dehydrogenation of C_8H_{12} species (ethyl-cyclohexadienes, methyl-ethyl-cyclopentadienes, and isomers) into C_8 aromatics and H_2 reduces the overall reactivity of the intermediate species pool by reducing the possibility of intermediate dehydrogenations, resulting in hydrogen atom formation.

As is typical for hydrocarbon fuels, at 1200 K, the reactivity is controlled by the $H + O_2 \rightarrow OH + O$ branching reaction. Also showing positive sensitivity are the hydrogen abstraction reactions from ethylene (C_2H_4) to form the vinyl radical (C_2H_3), which, because of the successive branching reaction $O_2 + C_2H_3 \rightarrow CH_2CHO + OH$, has a promoting influence on the overall reactivity. Abstraction reactions from decalin show negligible sensitivity, while the decomposition of $C_{10}H_{17}$ to pentadiene (C_5H_8) and hydrogen atoms has positive sensitivity. It is relevant to observe that, because of the large number of alternative decomposition paths, the overall reactivity is only slightly influenced by the kinetic parameters for a single decomposition path.

A similar scarce sensitivity of the overall reactivity was observed when separating the three primary isomers of $C_{10}H_{17}$ and also considering a more complete set of primary decomposition reactions.

On the contrary, at least a partial explanation of the overprediction of ignition delay times could be attributed to the low-temperature oxidation mechanism. Because of the similar cyclo-alkane structure, cyclohexane can be assumed as a reference fuel to quantify this possible effect. Cyclohexane was already extensively studied, both in the high- and low-temperature conditions.[38,39] In the same shock-tube operating conditions, it is possible to predict a reduction of ignition delay times of cyclohexane of ∼15−30%, when also considering the low-temperature mechanism. Of course, larger differences occur at low temperatures and high pressures. Further experimental and modeling research activities are needed to improve the model and to extend its reliability also at low temperatures.

Conclusions

New shock-tube measurements of decalin ignition delay times performed at elevated-pressure conditions are presented. The ignition times have been correlated using Arrhenius temperature dependence and power-law dependence on the pressure and equivalence ratio resulting in

$$\tau = 4.05 \times 10^{-9} P^{-0.78} \Phi^{-0.81} \exp(14930/T\,(\mathrm{K}))\ (\mathrm{s})$$

(37) Vanderover, J.; Oehlschlaeger, M. A. *Int. J. Chem. Kinet.* **2009**, *41*, 82–91.

(38) Granata, S.; Faravelli, T.; Ranzi, E. *Combust. Flame* **2003**, *132*, 533–544.

(39) Cavallotti, C.; Rota, R.; Faravelli, T.; Ranzi, E. *Proc. Combust. Inst.* **2007**, *31*, 201–209.

To our knowledge, the ignition time measurements presented here are the first ignition measurements for decalin at elevated pressures. A semi-detailed submechanism for decalin decomposition at the high-temperature conditions has been developed using an automatic kinetic generator, the MAMA program. Kinetic simulations are compared to the measured ignition times with adequate agreement. Sensitivity analysis indicates the limited importance of decalin unimolecular decomposition and hydrogen abstraction from decalin in predicting ignition times. The new decalin submechanism is a further step toward the improved kinetic understanding of pyrolysis and combustion of practical commercial fuels and surrogate mixtures.

Acknowledgment. The Rensselaer group was supported by the U.S. Air Force Office of Scientific Research (Grant FA9550-07-1-0114) with Dr. Julian Tishkoff as the technical monitor. The research activity of Politecnico was supported by the European Community in the behalf of the DREAM Project (FP7-211861). The authors also acknowledge the useful discussions with Prof. Tiziano Faravelli.

Appendix

MAMA program and product distribution from decalin decomposition.

A1. MAMA Program. The MAMA program is more than a simple automatic generator of a list of elementary reactions, it is also able to analyze reaction mechanisms and produce simplified or lumped reactions and mechanisms using lumped species and reactions (MAMA is not an acronym; it is only a Greek−Latin word meaning mother).

The schematic functions of the MAMA program are given in Figure A1. A mixture of radicals is exhaustively processed one by one by the isomerization and decomposition routines, which consider the possible isomerization and decomposition reactions and products. These routines may produce new radicals that are added to the radical list and new olefins or other unsaturated molecules that are added to a product list. Once all of the radicals have been analyzed, the elementary reactions and kinetic parameters that were used to analyze the possible isomerization and decomposition paths and the product species list are combined together, according to a pre-assigned model, to form an algebraic system that, once solved, gives the products list and their weights (distribution).

The functionality of the MAMA program is dependent upon some required inputs: (1) a "library of kinetic parameters" for the evaluation of the elementary reaction rate parameters, (2) a "proper molecule (radical/nonradical) description" for the representation of each species in the whole reaction path, (3) a "library of reaction types and rules", which lists the possible isomerization and decomposition reactions and the rules for evaluating rates and products, (4) a "proper reaction path" description, which enables the recognition of the reaction type, its products, as well as the sequence by which it is incorporated into the complete reaction path, (5) an "algorithm for molecule homomorphism", i.e., a nonambiguous and effective statement whether two molecule descriptions refer to the same product or not, and (6) a "numerical procedure", which starting from reactants, evaluates the reaction paths and distribution of final products. In doing so, the procedure should also offer the flexibility to implement different theoretical approaches, such as Rice and Herzfeld, Kossiakoff and Rice, or Dente and Ranzi.

In the field of automatic generation, most literature data and results are focused on the pyrolysis of linear and branched paraffins. In such situations, the complete set of species involved (intermediate and final) is limited to the order of hundreds. However, the pyrolysis of alkenes and cycloalkanes is much more complex. As an example, Figure A2 shows the number of intermediate and final species involved in the decomposition of these *n*-alkenes versus the carbon number of the *n*-alkene.

A similar complexity (number of species) is obtained for decalin and double-ring naphthenic compounds. The "explosive" growth in number of species with an increasing carbon number for naphthenes is due to ring opening and cyclization reactions, which generate new species without reducing the carbon number of the product from that of the reactant of a given reaction.

A detailed description of the functionalities, methodologies, and procedures of the MAMA program are exhaustively described by Dente et al. There, it is possible to find all details pertaining to the following features: (i) evaluation of end-product composition, (ii) lumping of components, (iii) database structure, and (iv) molecular homomorphism.

A2. Product Distribution from Decalin Decomposition. As discussed in the paper, the detailed kinetics of decalin decomposition would involve more than 75 000 reactions and more than 5500 species. Thus, it is evident that the results of a kinetic generator are of no practical use in the elementary form that they are obtained. It is neither of value nor of interest to perform kinetic simulations with several thousands of molecular species. It is more practical to "lump" the components with certain pre-assigned rules, which satisfy the requirements of the reactor model for which kinetic simulations will be performed. From a computing point of view, it can be conceptualized that a postprocessor is linked to the kinetic generator with the purpose of "lumping" the final products to a limited number of "pseudo" components.

Table A1. Influence of the Temperature on the Decomposition of Rdec1

	temperature (K)	1000	1050	1100
	reaction path	product distribution (weights)		
1a	$H + C_2H_4 + C_8H_{12}$	0.088	0.113	0.141
1b	$H + C_3H_6 + C_7H_{10}$	0.014	0.010	0.007
1c	$H + C_4H_8 + C_6H_8$	0.073	0.089	0.104
2a	$CH_3 + C_2H_4 + C_7H_{10}$	0.411	0.429	0.436
2b	$CH_3 + C_3H_6 + C_6H_8$	0.030	0.021	0.014
3a	$C_2H_5 + C_8H_{12}$	0.184	0.155	0.130
4a	$C_3H_7 + C_7H_{10}$	0.066	0.056	0.046
5a	$C_3H_5 + C_7H_{12}$	0.005	0.004	0.003
5b	$C_3H_5 + C_2H_4 + C_5H_8$	0.030	0.031	0.029
6a	$C_5H_7 + C_2H_4 + C_3H_6$	0.001	0.002	0.002
7a	$CyC_6H_9 + 2C_2H_4$	0.074	0.090	0.085
	total	0.977	0.999	0.998

Table A2. Influence of the Temperature on the Decomposition of Mix{$RC_{10}H_{17}$}

	temperature (K)	1000	1050	1100
	reaction path	product distribution (weights)		
1a	$H + C_{10}H_{16}$	0.025	0.029	0.032
1b	$H + C_2H_4 + C_8H_{12}$	0.033	0.041	0.050
1c	$H + C_3H_6 + C_7H_{10}$	0.011	0.009	0.007
1d	$H + C_4H_8 + C_6H_8$	0.037	0.046	0.056
1e	$H + C_4H_6 + C_6H_{10}$	0.012	0.011	0.010
2a	$CH_3 + C_4H_6 + C_5H_8$	0.117	0.093	0.074
2b	$CH_3 + C_2H_4 + C_7H_{10}$	0.109	0.113	0.115
2c	$CH_3 + C_3H_6 + C_6H_8$	0.024	0.018	0.013
2d	$CH_3 + 2C_2H_4 + C_5H_8$	0.032	0.026	0.021
2e	$CH_3 + C_4H_8 + C_5H_6$	0.040	0.047	0.054
3a	$C_2H_5 + C_8H_{12}$	0.123	0.110	0.096
3b	$C_2H_5 + 2C_4H_6$	0.018	0.016	0.014
4a	$C_3H_7 + C_7H_{10}$	0.064	0.064	0.062
5a	$C_3H_5 + C_7H_{12}$	0.075	0.075	0.075
5b	$C_3H_5 + C_2H_4 + C_5H_8$	0.012	0.016	0.020
5c	$C_3H_5 + C_3H_6 + C_4H_6$	0.011	0.009	0.007
6a	$C_4H_7 + C_6H_{10}$	0.069	0.082	0.095
6b	$C_4H_7 + C_2H_4 + C_4H_6$	0.017	0.024	0.027
7a	$2C_2H_4 + C_6H_9$	0.073	0.089	0.108

Table A3. Lumped Submechanism for Decalin Decomposition[a]

reaction	A	E_a (kcal/kmol)
Initiation		
decalin → cyC_6H_{10} + $2C_2H_4$	5.0×10^{16}	81000
decalin → $2aC_3H_5$ + $2C_2H_4$	1.0×10^{17}	78000
decalin → $2C_5H_8$ + 2H	1.0×10^{17}	78000
Dehydrogenation		
decalin → H_2 + 0.667decalin + 0.333tetralin	3.0×10^{13}	71000
Hydrogen Abstraction		
R + decalin → RH + $RC_{10}H_{17}$	16 secondary hydrogen atoms 2 tertiary hydrogen atoms	
Dehydrogenation of $RC_{10}H_{17}$		
$RC_{10}H_{17}$ → H + 0.667decalin + 0.333tetralin	1.0×10^{14}	39000
Decomposition of $RC_{10}H_{17}$		
$RC_{10}H_{17}$ → H + 0.5xylene + 0.5ethyl-benzene + H_2 + C_2H_4	4.4×10^{12}	30000
$RC_{10}H_{17}$ → H + toluene + H_2 + C_3H_6	8.4×10^{11}	30000
$RC_{10}H_{17}$ → CH_3 + 0.6$MecyC_6$ + 0.4indene + 0.6C_2H_4	5.2×10^{12}	30000
$RC_{10}H_{17}$ → CH_3 + toluene + H_2 + C_2H_4	4.55×10^{12}	30000
$RC_{10}H_{17}$ → CH_3 + C_4H_6 + C_5H_8	2.63×10^{12}	30000
$RC_{10}H_{17}$ → C_2H_5 + 0.5ethyl-benzene + 0.5xylene + H_2	6.0×10^{12}	30000
$RC_{10}H_{17}$ → C_2H_5 + $2C_4H_6$	7.8×10^{11}	30000
$RC_{10}H_{17}$ → C_3H_7 + 0.667toluene + 0.333$MecyC_6$	2.7×10^{12}	30000
$RC_{10}H_{17}$ → aC_3H_5 + 0.667$MecyC_6$ + 0.333toluene	2.85×10^{13}	30000
$RC_{10}H_{17}$ → aC_3H_5 + C_2H_4 + C_5H_8	2.15×10^{12}	30000
$RC_{10}H_{17}$ → pC_4H_7 + cyC_6H_{10}	2.5×10^{12}	30000
$RC_{10}H_{17}$ → pC_4H_7 + C_4H_6 + C_2H_4	1.25×10^{12}	30000
$RC_{10}H_{17}$ → cyC_6H_{11} + C_4H_6	1.25×10^{12}	30000

[a] Rate coefficients are given in the form $k = A \exp(-E_a/RT)$. Units are kmol, m, s, and kcal.

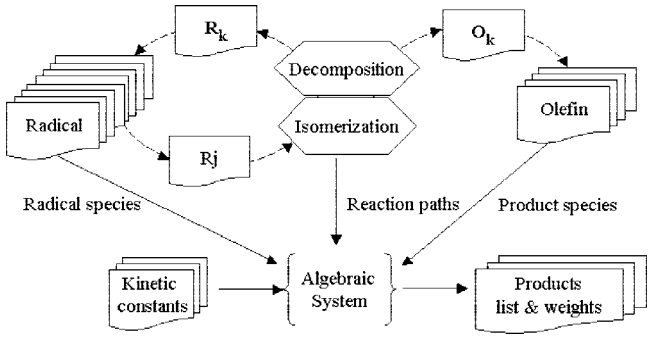

Figure A1. Schematic functions of the MAMA program.

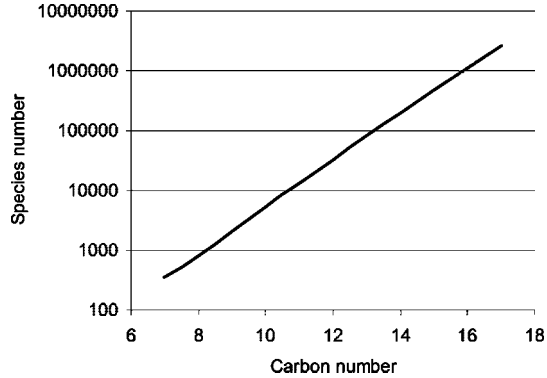

Figure A2. Number of species involved in the pyrolysis of *n*-alkenes versus the *n*-alkene carbon number.

Referring to the examples of radical decomposition discussed in the paper, Tables A1 and A2 show the influence of the temperature on the selectivities of the different decomposition paths of the Rdec1 and mix{$RC_{10}H_{17}$} radicals, respectively. Tables A1 and A2 give the lumped predictions of the MAMA program. These predictions have been lumped in terms of the different heavy components. For instance, the detail of the different C_7H_{10}, C_8H_{12}, $C_{10}H_{16}$ isomers, which the MAMA program reports, have been removed and replaced with lumped

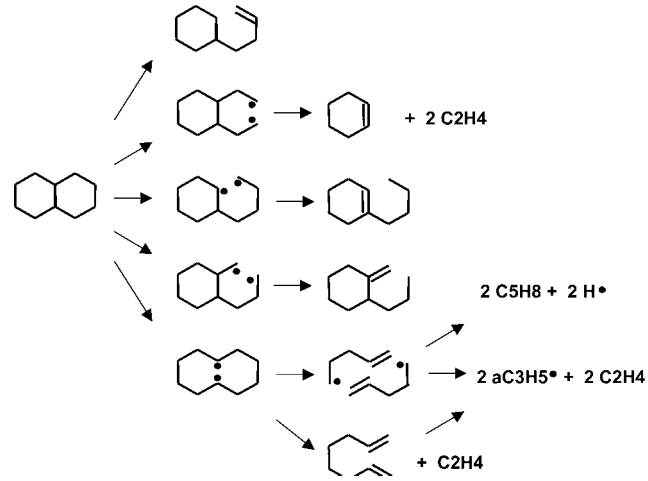

Figure A3. Molecular and radical initiation reactions for decalin.

species. The overall lumped kinetic scheme, given in Table A3, does not contain all of these intermediate species, and the lumping rules are used to describe the different reaction paths in terms of species already considered in the kinetic scheme. For example, the C_7H_{10} isomers are transformed into toluene and methyl-cyclohexane, at a ratio of 2:1, in the overall kinetic scheme. The C_8H_{12} isomers are directly dehydrogenated and transformed into H_2 and C_8 aromatics, because of the absence in the schemes of ethyl-cyclohexane, dimethyl-cyclohexane, and other alkyl-cycloalkanes isomers. Figure A3 shows several different decalin decomposition reactions, resulting in both molecular and radical products. Chae and Violi give a detailed discussion of decalin decomposition based on *ab initio* calculations. However, the sensitivity analysis has shown the small sensitivity of ignition delay at 1000 and 1200 K at 12 atm to decalin decomposition and also the small sensitivity to the different lumping assumptions in terms of the primary product distributions of decalin decomposition.

This lumped decalin mechanism is tied to the overall semi-detailed oxidation mechanism, which describes the fate of the decalin decomposition products. The complete kinetic scheme is available online at (www.chem.polimi.it/CRECKModeling/).

A3. References.

A1. Pierucci, S.; Ranzi, E. Comput. Chem. Eng. 2008, 32, 805−826.

A2. Rice, F. O.; Herzfeld, K. F. J. Am. Chem. Soc. 1934, 56, 284−289.

A3. Kossiakoff, A.; Rice, F. O. J. Am. Chem. Soc. 1943, 65, 590−595.

A4. Dente, M. E.; Ranzi, E. M. Mathematical Modeling of Hydrocarbon Pyrolysis Reactions; Academic Press, Inc.: New York, 1983; pp 133−174.

A5. Dente, M.; Bozzano, G.; Faravelli, T.; Marongiu, A.; Pierucci, S.; Ranzi, E. Kinetic modeling of pyrolysis processes in gas and condensed phase. In Advances in Chemical Engineering; Marin, G., Eds.; Elsevier, Inc.: Amsterdam, The Netherlands, 2007; Vol. 32, pp 52−166.

A6. Chae, K.; Violi, A. J. Org. Chem. 2007, 72, 3179−3185.

EF800892Y